Local probing of the giant magnetoresistance

S. J. C. H. Theeuwen,[a] J. Caro, S. Radelaar, L. Canali, and L. P. Kouwenhoven
Delft Institute of Microelectronics and Submicron Technology (DIMES), Delft University of Technology Lorentzweg 1, 2628 CJ Delft, The Netherlands

C. H. Marrows and B. J. Hickey
Department of Physics and Astronomy, University of Leeds, Leeds LS2 9JT, United Kingdom

(Received 6 June 2000; accepted for publication 10 August 2000)

We have contacted the tip of a scanning tunneling microscope (STM) to a Co/Cu magnetic multilayer to locally measure the giant magnetoresistance (GMR) of the multilayer. Apart from a point-contact GMR, the measured MR also reflects a magnetostriction effect in the STM. The resulting GMR ratios are typically 10%, with occasional ratios up to 60%. We attribute spot-to-spot variations of the ratio to differences in the local structure of the magnetic multilayer. © *2000 American Institute of Physics.* [S0003-6951(00)00641-0]

Recently, the giant magnetoresistance (GMR) of Co/Cu magnetic multilayers (MLs) has been studied using mechanical[1] and nanofabricated[2] point contacts. These contacts have a geometry intermediate between current-perpendicular-to-plane (CPP) and current-in-plane (CIP), so that their GMR should exceed the CIP GMR. However, the point-contact GMR ratio ($=\Delta R/R_{\mathrm{sat}}$, with ΔR the resistance change and R_{sat} the saturation resistance) is only about 5%, which is smaller than the corresponding CIP GMR ratio of the whole ML. It is not clear whether this low GMR is an intrinsic property of point contacts or GMR nanostructures in general, or due to dead layers at the bottom of the ML stack,[2] or damage introduced to the ML.[1,2] In this letter we use a scanning tunneling microscope (STM) to form point contacts to a GMR ML (inset Fig. 1) by very gently touching the tip to the high-quality top layers of the ML, thus avoiding the previous drawbacks. The small contact size combined with the scanning feature of the STM enable mapping of the local GMR of the ML.

The MLs comprise 25 repeats of a [Co(2 nm)/Cu(x nm)] period with $x=1$ or 2, corresponding to the first and second peak of antiferromagnetic coupling between the Co layers, respectively. They are deposited on a Si substrate with a Nb(100 nm)/Cu(4 nm) buffer and capped with a 3.4 nm($x=1$) or 2.4 nm($x=2$) thick Au layer to prevent oxidation.[3] Before making point contacts to these MLs, we perform CIP control measurements. These yield a regular in-plane field and perpendicular field GMR. The CIP GMR ratios of the MLs at 10 K (i.e., above T_c of Nb) and corrected for the parallel conductance of the Nb, are 30% and 20% for the first and second peak, respectively, irrespective of the field orientation.

The point contacts are made at 4.2 K by contacting the ML with a Au or Pt/Ir tip of a low temperature STM,[4] mounted in a magnet cryostat. The measurements are also at 4.2 K, where Nb is superconducting. Thus, the small CIP series resistance of the ML is completely shunted by the Nb, leaving only the point-contact contribution. The sample is mounted in the STM with the film plane perpendicular to or at an angle of 25° with the magnetic field, which is always parallel to the tip. This allows MR measurements in the perpendicular and approximately in-plane (further called in-plane) orientation of the ML. We first have contacted a 100 nm thick Au film with a Pt/In tip. The tip is moved towards the film, to a tunneling distance of about 0.5 nm to the surface. Then we switch off the feedback and gently touch the surface with the tip by tuning the piezo voltage. The contact resistance is controlled between several tens of mΩ and about 13 kΩ. While retracting the tip, we repeatedly observe conductance plateaus around values $n(2e^2/h)$, with $n=1-5$.[5] Further, point-contact spectra[6] display a clear phonon peak at the position characteristic of transverse acoustic phonons in bulk Au. This signature of ballistic electron transport, and the observation of conductance plateaus demonstrate our ability to controllably make clean contacts.

Contacts to both types of Au-capped MLs are made as described for Au films. We have made dozens of runs, contacting a fresh tip to a ML. In each run, many contacts with different resistances are made at different spots. We vary the

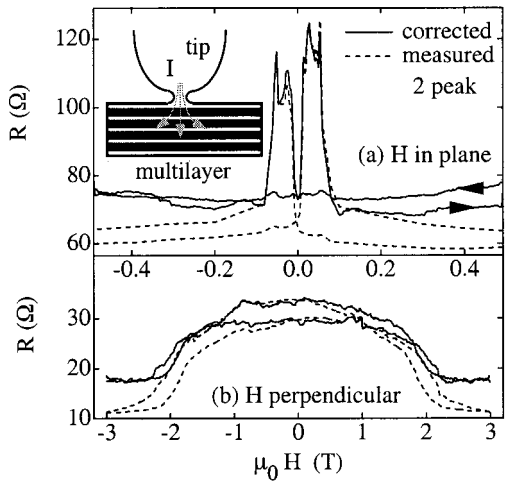

FIG. 1. Magnetoresistance of point contacts to a $[\mathrm{Co}(2\,\mathrm{nm})/\mathrm{Cu}(2\,\mathrm{nm})]_{25}$ multilayer for the in-plane (a) and perpendicular orientation (b). Dashed lines: as-measured curves. Solid lines: GMR after correction for magnetostriction. Inset: schematic cross section of a contact between tip and multilayer. The contact has a close-to-CPP geometry.

[a]Electronic mail: steven.theeuwen@philips.com

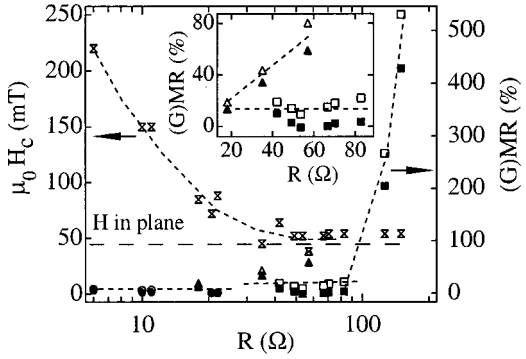

FIG. 2. (G)MR ratio (right-hand side axis) of $[Co(2\,nm)/Cu(2\,nm)]_{25}$ contacts vs saturation resistance for in-plane field orientation. Open symbols: measured. Solid symbols: corrected GMR. Corresponding coercive fields (left-hand side axis, hour-glass symbols) vs saturation resistance. Dashed line at 45 mT: coercive field of the CIP control GMR. Other lines guide the eye. Inset: expanded (G)MR for intermediate resistances.

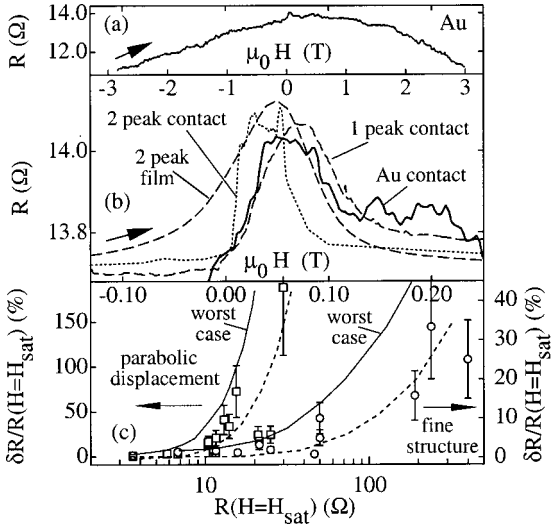

FIG. 3. (a) MR of a Au contact. (b) Fine structure in the MR of panel (a) together with (G)MRs, with scaled resistance values, representative of first- and second-peak contacts and of the second-peak film. (c) $\delta R/R(H=H_{sat}) = [R(H=0)-R(H=H_{sat})]/R(H=H_{sat})$ for Au contacts between 0–3 T (parabolic) and 0–0.1 T (fine structure) as a function of $R(H=H_{sat})$. Solid lines: worst-case estimate, used as correction. Dashed lines guide the eye.

resistance at one spot by moving the tip with the *z*-piezo, resulting in what we call a sequence of resistances. Often the contact MR is flat, in spite of careful contacting. Nevertheless, enough contacts yield a MR with characteristics of a GMR. The MR ratio is typically in the range 1%–80% for resistances below 80 Ω, reaching for this type of ML unprecedented values of several hundred percent for resistances above 80 Ω. These high values are reminiscent of the recently reported very large MR of atomic size Ni–Ni contacts,[7] which is attributed to an abrupt domain wall. The behavior of the MR ratio versus contact resistance shows a stronger scatter for MRs taken from different spots than for a sequence of MRs from a single spot. We relate part of this scatter to the variation of the ML quality, e.g., spread in layer thickness, interface roughness, and relative alignment of the magnetization of the Co layers at $H=0$. The variation is resolved due to the small contact size and limited probing depth, implying absence of averaging over a large area and many bilayers.

MRs coming from two sequences of contacts to a second-peak ML are shown in Figs. 1(a) and (b) (dashed lines), for the in-plane and perpendicular orientation. The field scale and hysteresis of the MRs are consistent with those of the CIP control GMR. The MR ratios are 80% for Fig. 1(a) and 200% for Fig. 1(b), both larger than the CIP GMR ratio. In Fig. 2, we plot for second-peak contacts the in-plane MR ratio versus the resistance in saturation, which is the better defined magnetic state. The open symbols are points for as-measured curves. The square and triangular symbols represent two sequences, the point at 57 Ω corresponding to the curves of Fig. 1(a). Circular symbols (below 25 Ω) represent contacts at different spots. As can be seen, for $R<25\,\Omega$ (diameter >10 nm) the ratios are small ($\approx 5\%$), which we attribute to damage in the ML, due to the indentation of the tip. In this range, the coercive field increases strongly with decreasing resistance, as shown in Fig. 2 (left-hand side axis). In the range of 40–80 Ω, the coercive field saturates close to the film value (45 mT). This means that small indentations by the tip affect the ML only weakly. In this range, the MR ratios varying between 10%–80% (inset Fig. 2). Above 80 Ω (diameter <3 nm) a strong increase of the MR ratio sets in, reaching a huge value of 530%.

Globally, contacts to first-peak MLs behave similarly. They also show a strong increase of the MR ratio above an onset resistance, even up to values above the maximum second-peak MR ratio. Among the sequences, the onset resistance varies in the range of 5–60 Ω. Further, the MR of these contacts has a saturation field of 200 mT instead of 2 T for the CIP-control GMR. This may arise from the weaker coupling of the top Co layer, which is only exchange coupled to one Co layer, giving a smaller saturation field. However, we believe that the deviating field scale and the turn up to large MR ratios with increasing contacts resistance have an origin extrinsic to the ML, involving the effect of a magnetic field on the STM.

These contacts are very sensitive to a small displacement of the tip relative to the film, so that a field-dependent displacement intrinsic to the STM may play a role. To check this, we measure the MR of contacts to a Au film, which should be much weaker[8] than the effect in Fig. 2. The resulting MRs are negative, parabola-like, and, most importantly, large (up to 200%). This is exemplified in Fig. 3(a). We interpret this resistance change as a field-dependent deformation of parts of the STM, resulting in increasing indentation of the film by the tip with increasing field, and thus a lower resistance. This agrees with the increasing tunnel current with increasing magnetic field measured in tunneling mode of the STM. We attribute the deformation to magnetostriction of the STM, which is a length change when it becomes magnetized.[9] The STM apparently has parts with residual magnetism, although its materials are qualified as nonmagnetic. The Au contact senses the magnetostriction, so that the ordinate of Figs. 3(a), (b), and (c) actually represents magnetostriction. Thus, part of the ML contact MR arises from this displacement effect. The magnetostriction effect due to the ML itself is negligible.[9]

The field scale of the overall displacement effect in Fig. 3(a) is comparable to that of the MR of Fig. 1(b) and much larger than the MR of Fig. 1(a). Thus, the overall displace-

ment can strongly affect the perpendicular GMR, but can hardly alter the in-plane GMR. More serious for the latter, however, is the fine-structure present in the curve of Fig. 3(a) close to $H=0$. This fine structure, plotted in Fig. 3(b) on an expanded scale, together with scaled MRs representative of first- and second-peak contacts of intermediate resistance ($40\,\Omega<R<80\,\Omega$), has a hysteretic maximum at about 55 mT, independent of the contact resistance. The fine structure corresponds to a displacement of about 0.4 nm, as deduced from the piezo-voltage change of its tunneling-mode counterpart. Quite incidentally, the field position and shape of the fine structure are very similar to those of the MR of the first-peak contacts [Fig. 3(b)]. This indicates that the MR of the first-peak contacts mainly originates from the displacement. However, such a strong similarity does not hold for the fine structure and the MR of the second-peak contacts, which are clearly separated [Fig. 3(b)]. Rather, the field position of the second-peak contact is very close to the peak of the CIP GMR, while its shape is clearly narrower. The latter property agrees with absence of averaging over many domains in a point-contact MR. Under the reasonable assumption of a unique field scale of the displacement effect, part of the second-peak-contact MR thus is GMR. Apparently, the second-peak contacts are less sensitive to the displacement, which is probably related to the different few top layers (2 nm Cu/2.4 nm Au instead of 1 nm Cu/3.4 nm Au). The conclusion that part of the MR is GMR agrees with the peak-position (coercivity) increase for $R<25\,\Omega$ in Fig. 2, which is absent for Au contacts. The coercivity increase is caused by destruction of the exchange coupling between neighboring Co layers due to indentation-induced damage in the ML. For the two resistances above 80 Ω, the MR maximum has shifted to the fine structure of the Au contacts. This means that the MR is increasingly caused by the displacement effect.

To correct the MR of the second-peak contacts for the displacement, a calibration of this effect specific for a second-peak ML with a 2.4 nm Au cap is needed. Such a calibration being inaccessible, we use the MR of the Au contacts for this purpose. Their parabola-like MR and fine structure, $\delta R/R(H=H_{\mathrm{sat}})=[R(H=0)-R(H=H_{\mathrm{sat}})]/R(H=H_{\mathrm{sat}})$ are plotted as a function of $R(H=H_{\mathrm{sat}})$ in Fig. 3(c). Here, H_{sat} is the saturation field of the ML-contact MR for the in-plane ($\mu_0 H_{\mathrm{sat}}=0.1\,\mathrm{T}$) or perpendicular ($\mu_0 H_{\mathrm{sat}}=3\,\mathrm{T}$) geometry. $\delta R/R(H=H_{\mathrm{sat}})$ increases strongly with increasing resistance, which agrees with the intuitively expected stronger relative change of the contact area per unit tip displacement for smaller contact areas. This behavior is similar to that of the MR in Fig. 2, emphasizing the role of the displacement. To correct the MR ratios of Fig. 2 we use the worst-case line through the error bars of $\delta R/R(H=H_{\mathrm{sat}})$ [Fig. 3(c)]. We add the interpolated δR to the saturation resistance of the ML point-contact MR to obtain the GMR ratio. This correction overestimates the displacement, since for the same resistance the diameter of a Au contact is smaller than that of a ML contact.[10] GMR curves are obtained by subtracting a Au-contact MR curve with a scaled amplitude equal to the corresponding δR of the worst-case estimate.

In Fig. 2, the filled symbols denote the GMR ratios. The ratio is $\leqslant 5\%$ for $R<25\,\Omega$, where the signal is mainly GMR. For the other extreme, $R>80\,\Omega$, we find strongly enhanced ratios of over 200%. Large GMR ratios are very well possible for the mixed CIP/CPP geometry of the contacts in combination with a good local magnetic structure. However, this does not explain the enhancement. Although the enhancement may be due to a size effect, e.g., collimation,[11] it is more likely to arise from inadequacy of the correction procedure for $R>80\,\Omega$. In this range, which is somewhat limited in Fig. 3(c), the resistance is most sensitive to displacement, and the field position of the ML contacts MR has shifted towards the fine structure of the displacement. For intermediate resistances $40\,\Omega<R<80\,\Omega$, on the contrary, a GMR must remain after correction because of the field-scale arguments discussed in the context of Fig. 3(b). The two sequences studied in detail in this range behave differently (see inset Fig. 2). For one sequence, the GMR ratio takes values up to 10%, while for the other, it increases with resistance up to 60%. The in-plane GMR curve corresponding to the 60% point is the solid line in Fig. 1(a), while the solid line in Fig. 1(b) is the corrected perpendicular GMR with ratio 90%. The resulting GMR ratio in the intermediate resistance range have to be rather accurate, since the GMR after correction saturates, as illustrated in Fig. 1.

In conclusion, we have measured the MR of point contacts made by contacting the tip of an STM to a Co/Cu multilayer. Part of the MR is a magnetostriction effect in the STM, which dominates for contacts to first-peak MLs, but leaves a clear GMR for contacts to second-peak MLs. For the latter, restricting ourselves to sequences of resistances measured at a spot, we obtain GMR ratios up to 60%, depending on the local quality of the ML.

[1] M. V. Tsoi, A. G. M. Jansen, and J. Bass, J. Appl. Phys. **81**, 5530 (1997).
[2] K. P. Wellock, S. J. C. H. Theeuwen, J. Caro, N. N. Gribov, R. P. van Gorkom, S. Radelaar, F. D. Tichelaar, B. J. Hickey, and C. H. Marrows, Phys. Rev. B **60**, 10291 (1999).
[3] C. H. Marrows, N. Wiser, B. J. Hickey, T. P. A. Hase, and B. K. Tanner, J. Phys.: Condens. Matter **11**, 81 (1999).
[4] J. Wildoër, thesis, TU Delft, 1996.
[5] A. I. Yanson, G. R. Bollinger, H. E. van den Brom, N. Agrait, and J. M. van Ruitenbeek, Nature (London) **395**, 783 (1998).
[6] P. A. M. Holweg, J. Caro, A. H. Verbruggen, and S. Radelaar, Phys. Rev. B **45**, 9311 (1992).
[7] N. García, M. Muñoz, and Y.-W. Zhao, Phys. Rev. Lett. **82**, 2923 (1999).
[8] P. A. M. Holweg, J. A. Kokkedee, J. Caro, A. H. Verbruggen, S. Radelaar, A. G. M. Jansen, and P. Wyder, Phys. Rev. Lett. **67**, 2549 (1991).
[9] See e.g., R. M. Bozorth in *Ferromagnetism* (Van Nostrand, Toronto, 1951), who also reports that the magnetostriction of Co is $\approx 10^{-5}$. For the 50 nm thick Co in the ML the thickness change thus is 0.5×10^{-3} nm.
[10] We estimate the contact diameter from the resistance R using Wexler's formula [G. Wexler, Proc. Phys. Soc. **89**, 927 (1966)] $d=(\rho_{\mathrm{tip}}+\rho_x)/4R+1/R\cdot\sqrt{(\rho_{\mathrm{tip}}+\rho_x)^2/2+16/3\pi R(\rho l)_x}$ with ρ_{tip} the resistivity of the tip and ρ_x that of the Au or ML film and l the mean free path. $\rho l\approx 1\ \mathrm{f\Omega m^2}$ [J. Bass, *Landolt Börnstein New Series*, (Springer, Berlin, 1982), vol. III/15a], and $\rho_{\mathrm{ML}}/\rho_{\mathrm{Au}}\approx 20$, so that $d_{\mathrm{ML}}/d_{\mathrm{Au}}=1-20$.
[11] Collimation is a narrowing of the angular injection distribution, a known effect in ballistic constrictions in GaAs [C. W. J. Beenakker and H. van Houten, Solid State Phys. **44**, 1 (1991)]. For neck-shaped ML constrictions collimation not only leads to a stronger CPP-like current, but also to a higher probability of backscattering through the orifice for specular scattering at the interfaces. A collimated current along specific crystallographic directions leads to enhanced reflection probabilities, and thus, an enhanced GMR.